

Experimental Results of Unbiased Control of 9-Pole Radial Magnetic Bearing

Myounggyu D. NOH^a, Wonjin JEONG^a, Miseon SONG^a

^a Dept. Mechatronics Engineering, Chungnam National University, 99 Daehak-ro, Yuseong-gu, Daejeon, Korea, mnoh@cnu.ac.kr

Abstract

Previously, a generalized unbiased control strategy has been proposed for unsymmetrical radial magnetic bearings, which reduces the risk of slew rate limiting. In this paper, nine-pole radial bearings are designed and applied them to an industry-scale compressor prototype. The bearing is configured so that a single inverter can drive one radial bearing. In order to implement the control laws, phase selection algorithm is examined. When the force inversion rule is included in the plant dynamics, it is found that the plant seen by the controller is linear. Lead-filter type control laws are designed and implemented. Measurements of the sensitivities confirm the appropriateness of the control.

Keywords: Unsymmetrical bearing, Unbiased control, Force inversion, Phase selection

1. Introduction

Typical radial active magnetic bearings are structurally symmetric. For example, an eight-pole bearing uses two opposing pairs to control one axis by winding two adjacent poles in series. Each pole pair is driven by a power amplifier. Bias linearization is widely used to overcome the quadratic relationship of coil currents to the magnetic force. However, the bias currents increase the ohmic losses and require larger capacity of power amplifiers that are needed to supply control currents.

Unbiased control of symmetric bearings has the critical issue of slew rate limiting (Tsiotras & Wilson 2003). Unsymmetrical three-pole bearings have been studied as well (Chen & Hsu 2002, Hemenway & Severson 2020). However, they are applicable to very small rotors and the control axes are cross-coupled.

A generalized unbiased control strategy for unsymmetrical bearings has been proposed by Meeker (Meeker 2017). The strategy reduces the risk of slew rate limiting. Also, it is possible to use linear control law, if the nonlinearities are handled inside the plant dynamics.

In this research, we have applied the unbiased control strategy to active magnetic bearings supporting an industry-scale compressor. The performance of the control is investigated through experiments.

2. Unbiased Control Strategy

2.1 Current to Force Relationship

The 9-pole radial magnetic bearing considered in this paper is illustrated in Figure 1. The reference axes and pole numbering are also shown. As discussed in Meeker (2017), all nine poles can be independently driven by three inverters with the possibility of fault tolerance. In this paper, however, three adjacent poles are grouped so that a single inverter can drive the bearing.

Using magnetic circuit analysis, the forces that are generated by coil currents can be expressed as

$$f_x = \frac{1}{2} \mathbf{i}^T \mathbf{M}_x \mathbf{i}, \quad f_y = \frac{1}{2} \mathbf{i}^T \mathbf{M}_y \mathbf{i} \quad (1)$$

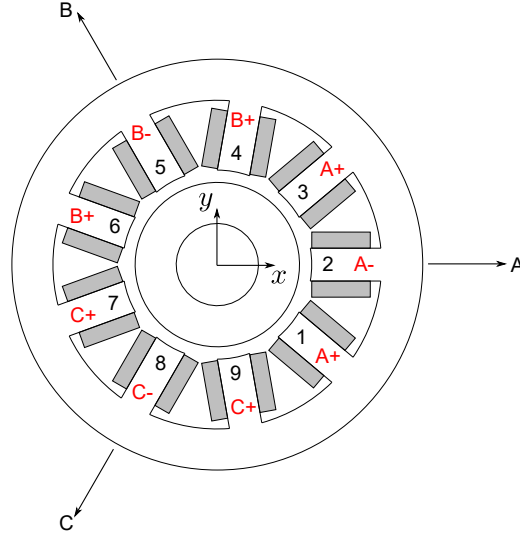


Figure 1: Schematic of 9-pole radial bearing

where \mathbf{i} is the vector of coil currents and defined as $[i_A \ i_B \ i_C]^T$. In (1), \mathbf{M}_x and \mathbf{M}_y are the matrices determined by bearing geometry. Since two-dimensional forces are determined by three currents, the force-current relationship in (1) is not unique. Suppose that two independent currents, i_r and i_i , arranged in a complex form satisfy

$$f = f_x + jf_y = (i_r + ji_i)^2 \quad (2)$$

Then, the forces can be determined by

$$f_x = i_r^2 - i_i^2, \quad f_y = 2i_r i_i \quad (3)$$

Since the mapping from the control currents to coil currents is not unique, a constrained optimization can be set up to find the mapping matrix, where the elements of the matrix and the total flux in the bearing are minimized (Meeker 2017). The mapping matrix for a nine-pole bearing with three adjacent poles wired in series is given as

$$\mathbf{W} = \begin{bmatrix} 1.02623 & 0 \\ -0.51312 & -0.88874 \\ -0.51312 & 0.88874 \end{bmatrix} \quad (4)$$

with respect to the reference axes in Figure 1.

The force-current relationship (1) does not account for the dependence of the force with respect to the position of rotor. The control currents must be adjusted in order to include the position dependence as follows (Meeker 2017):

$$i_r^* = i_r - xi_r - yi_i, \quad i_i^* = i_i + xi_i - yii_r \quad (5)$$

where x and y are the displacements of the rotor.

2.2 Force Inversion and Phase Selection

Figure 2 shows the block diagram of unbiased control. Control law generates the required force of f_x^* and f_y^* . The required control currents can be obtained by inverting the force-current relationship.

$$i_r = \frac{1}{\sqrt{2}} \sqrt{|f| + f_x}, \quad i_i = \frac{\text{sgn}(f_y)}{\sqrt{2}} \sqrt{|f| - f_x} \quad (6)$$

where

$$|f| = \sqrt{f_x^2 + f_y^2}$$

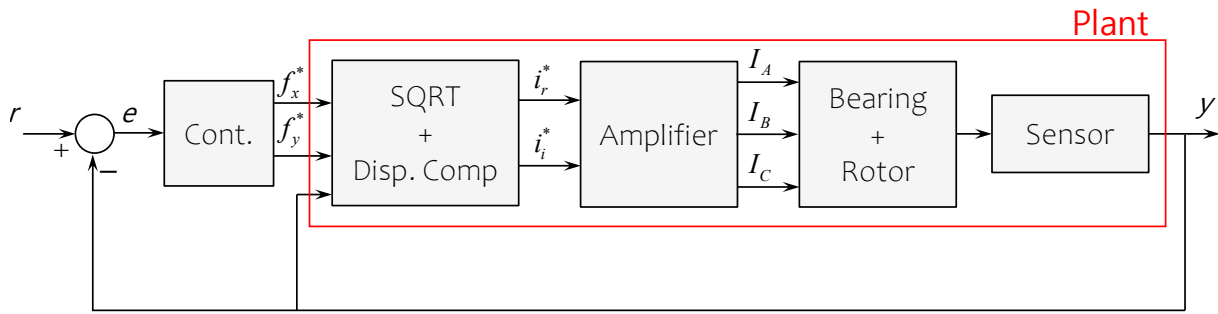


Figure 2: Block diagram of unbiased control

When inverting the force-current equation, it is important to avoid discontinuity in current outputs. As shown in Figure 3, there can be a large jump in i_r when the force command crosses the negative real axis (from F_1 to F_2). If the phase of the current is adjusted by π as in the right diagram, the continuity of the control current can be maintained.

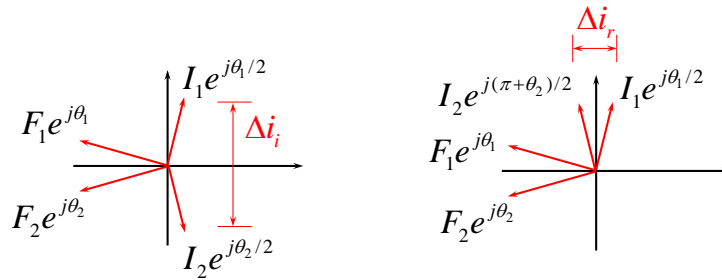


Figure 3: Phase selection

If we treat the force inversion and the displacement compensation as a part of the plant, this plant seen by the force command is linear. Therefore, typical control laws such as lead filters can be used to levitate the bearing.

3. Test Rig for Unbiased Control

Two Nine-pole radial AMBs (motor side and impeller side) are designed to support a chiller compressor (capacity of 500RT and the operating speed of 18,000 rpm). The load capacity of each bearing is 1120 N. Journal diameter is 93.2 mm. The pictures of the compressor and the bearing are shown in Figure 4.



Figure 4: Prototype of chiller compressor and 9-pole radial AMB

Lead filter type control laws are used. Notch filters are employed to suppress the vibration due to flexible modes. Integrators are added to decrease the steady-state error. Figure 5 shows the bode plots of the controllers for motor and impeller bearings.

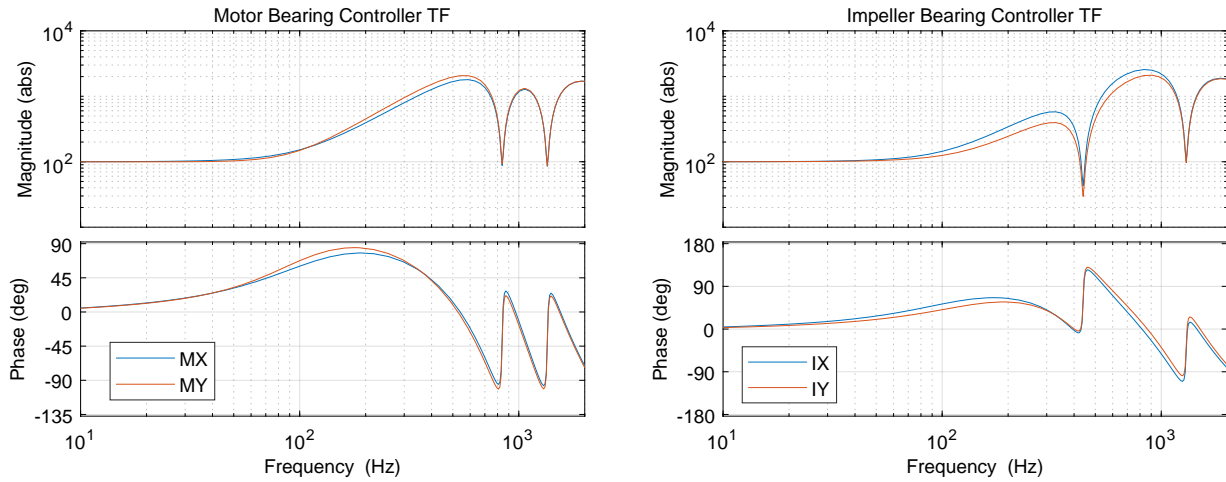


Figure 5: Bode plots of control transfer functions for motor and impeller bearings

4. Test Results

Levitation control is implemented using MATLAB/SimulinkRT at the sampling rate of 10 kHz. Plant transfer functions and output sensitivities are measured through sine sweep tests. The plant transfer functions are shown in Figure 6. The output sensitivities are shown in Figure 7. Measured sensitivities satisfy ISO14839-3 requirements.

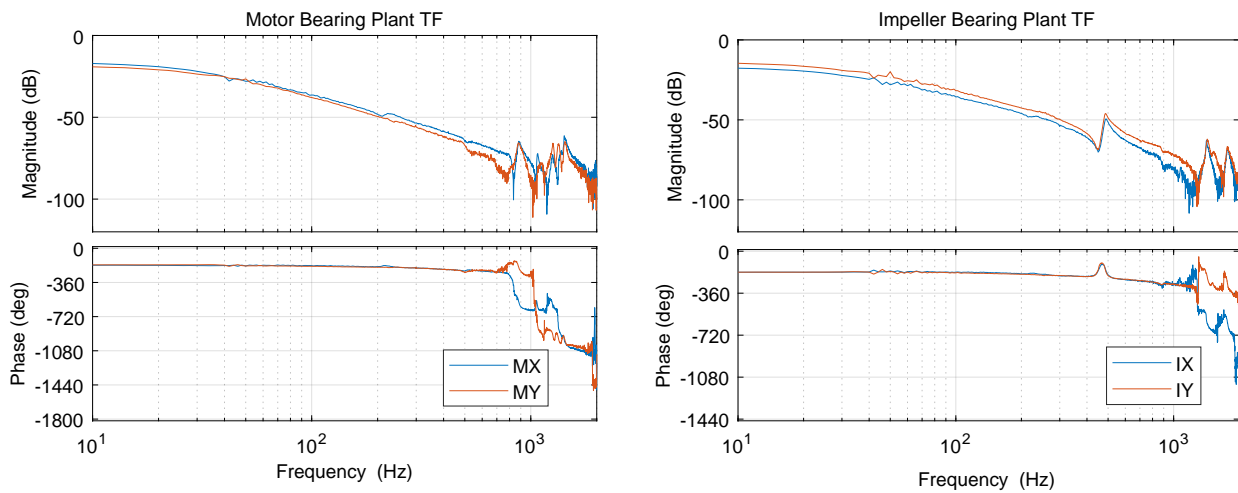


Figure 6: Plant transfer functions of motor and impeller bearings

References

Chen, S.-L. & Hsu, C.-T. (2002), 'Optimal design of a three-pole active magnetic bearing', *IEEE Transactions on Magnetics* **38**(5), 3458–3466.

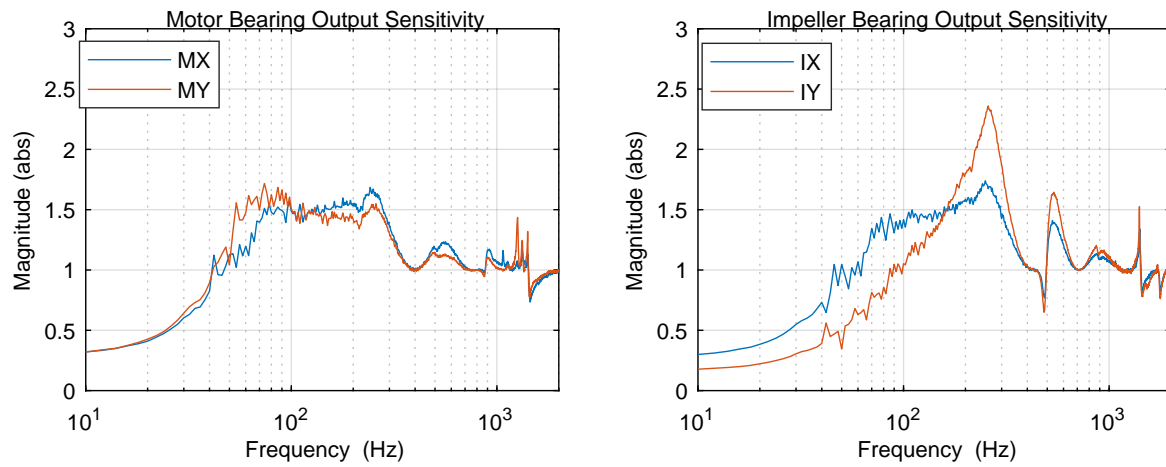


Figure 7: Sensitivity measurements for motor and impeller bearings

Hemenway, N. R. & Severson, E. L. (2020), 'Three-pole magnetic bearing design and actuation', *IEEE Transactions on Industry Applications* **56**(6), 6348–6359.

Meeker, D. (2017), A generalized unbiased control strategy for radial magnetic bearings, in 'Actuators', Vol. 6, MDPI, p. 1.

Tsiotras, P. & Wilson, B. C. (2003), 'Zero-and low-bias control designs for active magnetic bearings', *IEEE Transactions on Control Systems Technology* **11**(6), 889–904.